

# Impact of Detailed Fuel Chemistry on Knocking Behaviour in Engines

Roger F. Cracknell<sup>1</sup>✉, Arjun Prakash<sup>2</sup>, Kieran P. Somers<sup>1,4</sup>, and Chongming Wang<sup>3,5</sup>

<sup>1</sup> Shell Global Solutions, Manchester, UK  
Roger.Cracknell@shell.com

<sup>2</sup> Shell Global Solutions, Houston, USA

<sup>3</sup> Shell Global Solutions, Hamburg, Germany

<sup>4</sup> National University of Ireland, Galway, Ireland

<sup>5</sup> University of Birmingham, Birmingham, UK

**Abstract.** Demand for more efficient gasoline vehicles has driven the development of downsized, engines, which benefit from higher octane.

Features on modern SI engines such, direct injection, inter-cooling in boosted engines, cooled EGR and Millerisation lead to a much lower temperature for a given pressure in a real engine as compared to the test conditions in the CFR engine used to define the Research Octane Number (RON) and Motor Octane Number (MON) octane rating scales.

Because the end-gas in modern engines experiences a different pressure/temperature history during knocking cycles, as compared to the CFR engine, there is a growing body of evidence to suggest that for a given RON, it may actually be beneficial to have a high octane sensitivity (RON-MON) or in other words a lower MON.

To explore this further, tests have been conducted in a single cylinder DISI engine over the whole speed load map using three different compression ratios, and fuels with two different levels of RON but with three octane sensitivity levels ranging from 5 to 15. These results have been further interpreted by reference to chemical kinetic models for gasoline autoignition, which can be used to rationalise how the influence of sensitivity varies over the speed/load map.

## 1 Introduction

Driven by increasing market demands for higher fuel efficiency, gasoline engines have drastically increased in complexity over the past two decades to incorporate direct injection (DI), turbocharging, cylinder deactivation, intercooling and EGR. Fuel octane quality can play a significant role in improving engine efficiency, through preventing knock, and hence allowing the engine to operate close to optimal spark timing [1–4].

Octane is defined using two industry standards: RON and MON, which are measured on a single-cylinder standardized naturally aspirated carburettor engine designed in 1929, known as the Cooperative Fuel Research (CFR) engine [5, 6]. The octane quality of an actual fuel is defined in terms of the volume fraction of iso-octane in a Primary

Reference Fuel (PRF) consisting of iso-octane and n-heptane which has the same knocking characteristics as the real fuel.

The auto-ignition characteristics of PRF fuels are different to real-world gasolines. Figure 1 illustrates the ignition delay time as a function of temperature for a surrogate “real fuel” and two PRF mixtures, where PRF95 denotes a mixture with 95% by volume of iso-octane and 5% by volume of n-heptane, which has an octane number of 95 and PRF85 is defined in an analogous fashion. Such a plot is familiar from experimental techniques such as rapid compression machines and shock tubes.

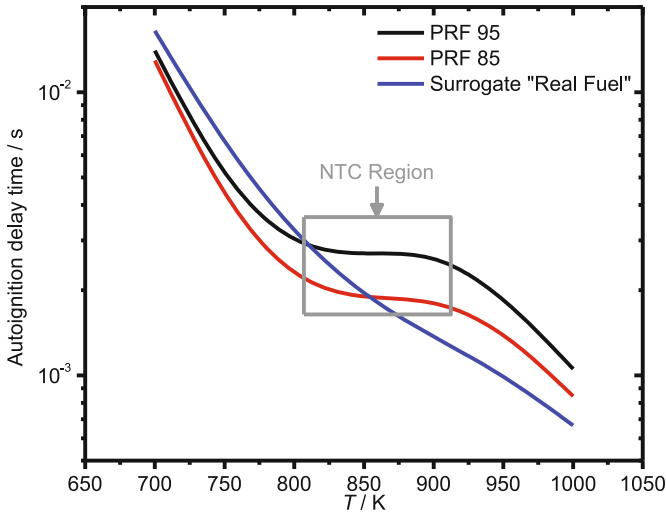


**Fig. 1.** Calculated autoignition delay times at 40 atm for a surrogate gasoline comprising 62 vol. % toluene, 16 vol. % i-octane, 22 vol. % n-heptane (95 RON, 85 RON), PRF95, and PRF85. Surrogate compositions were computed based on the work of [7]. All simulations were carried out for stoichiometric fuel in air ( $\phi = 1$ ) mixtures using the chemical kinetic mechanism from [8].

For the surrogate “realistic” gasoline, the autoignition delay time decreases monotonically with increasing temperature. By contrast the PRF fuels show a “Negative Temperature Coefficient” (NTC) region in which the ignition delay does not decrease with increasing temperature.

Approaching the NTC region, the line for the surrogate “real fuel” crosses over the curve for PRF 95 and then at higher temperatures it crosses the curve for PRF 85. The temperatures at which the surrogate intersects the PRF 95 and PRF 85 curves respectively can be thought of as representing the conditions in the RON and MON tests because the ignition delay of the real fuel and the PRF defining the octane number are the same. The presence of the pronounced NTC behaviour in the primary reference fuels is the main reason why the RON of a real fuel is typically around 10 numbers higher than the MON. At temperatures, lower than the NTC region, the surrogate “realistic” gasoline is more resistant to autoignition than either PRF 95 or PRF 85. If the engine operates in a regime of pressure -temperature space such that it is more resistant to

autoignition than its RON value, then the engine is said to be operating in the “beyond RON” region [9–11].

A practical approach developed by Kalghatgi [9, 10] to quantify the octane appetite of modern engines is to define an octane index (OI) as a linear combination of RON and MON with an engine condition dependent weighting factor, K, such that

$$\text{OI} = K \times \text{MON} + (1 - K) \times \text{RON}. \quad (1)$$

This can also be written as

$$\text{OI} = \text{RON} - KS, \quad (2)$$

where S is the sensitivity (RON-MON). The K value is dependent only on the in-cylinder temperature and pressure conditions in the end-gas prior to the onset of auto-ignition.

Most investigations into the effects of octane index have found that modern engines exhibit negative K values when operating at near-knocking conditions [4]. A negative K value means that the engine will be more knock resistant using fuels with a higher RON and a higher sensitivity [4]. It has however been noted that the K value can be different at different regions of the speed load map and where the acceleration follows different trajectories. Many authors have reported that K decreases with increased engine load and intake pressure [9–15]. This can be rationalised in terms of Fig. 1 because higher intake pressure in a boosted engine with intercooling, means that the temperature for a given pressure will be lower, pushing the combustion regime further “beyond RON” in the left of Fig. 1. Other authors have also reported that the value of K increases with engine speed [4, 9, 16].

To explore this further, tests have been conducted in a single cylinder DISI engine over the whole speed load map using three different compression ratios, and fuels with two different levels of RON but with three octane sensitivity levels ranging from 5 to 15. The detailed results of these experiments are reported elsewhere [3, 18].

In this work, these results have been further interpreted by reference to chemical kinetic models for gasoline autoignition combined with a 0D engine model, which can be used to rationalise how the influence of MON varies over the speed/load map.

**Table 1.** Fuel matrix properties

	RON	MON	Density (kg/m <sup>3</sup> )
F1	92	87	718.0
F2	92	82	742.3
F3	92	78	731.1
F4	98	93	698.6
F5	98	88	730.0
F6	98	83	749.0

## 2 Single Cylinder Engine Testing

### 2.1 Fuel Matrix

The six fuels tested are reported in Table 1. They all contain approximately 10% ethanol by volume and were blended in Shell Technical Centre Hamburg (STCHA) without any deposit control additives or other performance boosting additives. Given the study's focus on octane sensitivity, the fuels are split into two subsets of constant RON but varying MON. F2 is representative of regular grade gasoline in the North American market while F5 represents premium grade in the same market. The properties of all fuels were tested using standard methods before being transferred to the single cylinder engine.

### 2.2 Experimental Facilities and Single Cylinder Engine

A 4-stroke single-cylinder AVL DISI research engine was used to carry out all testing. The Compression Ratio (CR) of the engine can be varied between 9.5:1, 10.5:1 and 11.5:1 by inserting metal sheets of varying sizes between the cylinder liner and crankcase; these are denoted CR1, CR2 and CR3 respectively. The 4-valve pent-roof cylinder head with centrally mounted piezo direct injector and Variable Valve Timing (VVT) system for all four valves make up the engine's combustion system. The spark plug was centrally located within the combustion chamber.

An electric dynamometer was used to maintain the engine operating at a constant speed ( $\pm 1$  RPM) for all power outputs. Real time combustion indication and analysis was achieved using an AVL Indicom system. An IAV FI2RE management system was used to control the engine. A Siemens CATs system controlled the fuel, air, coolant, oil conditioning units and emissions measurement equipment during operation. The CATs system also carried out signal acquisition and recording during the engine's operation.

The in-cylinder pressure was measured using a Kistler pressure transducer, installed in a sleeve on the intake and exhaust bridge. A charge amplifier (ETAS ES630.1) was used to collect pressure measurements. In the range between 30° and 70° CA After Top Dead Centre (ATDC) the data was recorded at a resolution of 0.1° CA, in the remaining range at a resolution of 1° CA.

Boosted air (up to 3 bar) was delivered to the engine using a connected external air handling device. Before entering the engine, the air was dried, filtered and delivered to a 200L conditioning unit where the air pressure and temperature were tightly controlled using a closed-loop approach. The engine was operated with stoichiometric combustion with any fuel volumetric energy content differences compensated through the injector pulse width. An AVL fuel mass flow meter was used to control fuel consumption and individual AVL conditioning systems controlled the fuel, coolant and lubricant during engine operation.

### 2.3 Experimental Procedure

In the first experimental phase, F2 and CR3 (11.5) were used to determine the engine's optimization parameters such as optimum injection mapping and valve timings. These

remained unchanged throughout all testing thereafter. In the second phase F1-F6 were tested for all compression ratios at a number of speed-load conditions, described in Table 2. Tests for F2 CR2 (10.5) were repeated at the start, middle and end of the procedure to verify consistency of results.

**Table 2.** Speed-Load conditions tested

Engine Speed (RPM)	Engine IMEP (bar)
1000	2, 4, 6.5, 8, 9.5, 12, 14, 16
1800	2, 4, 6.5, 8,
2500	9.5, 12, 14,
3500	16, 18, 20, 22

Before each experimental set-up, the fuel system was flushed with the new sample and the compression ratio was manually adjusted as previously described. An engine warm up period of about 30 min was required to warm up oil and coolant to temperatures of 360 K and 355 K respectively. Engine leakage was monitored and oil dilution checked using hydrocarbon emissions data. Daily engine operating check points were performed to ensure correct operation of all measurement systems and engine, after which the testing protocol begun.

With each testing condition the spark timing was gradually advanced until MBT was reached, estimated by placing MFB50 at  $7.5 \pm 0.5^\circ$  ATDC. In some cases the onset of knock prevented reaching MBT advance and the testing was carried out in Knock-Limited Spark Advance (KLSA). At 1800 RPM the tolerated threshold for engine knock was 2 bar cycle-based maximum in-cylinder pressure oscillation. The CATs software was used to take 10 Hz measurements for in-cylinder, exhaust and intake pressures as well as ignition and injection signals, which were recorded onto the AVL Indicom system every 100 cycles.

## 2.4 Impact of Octane Sensitivity on Thermal Efficiency

Indicated thermal efficiency can be obtained from the indicated specific fuel consumption measurements and an efficiency map plotted. Maps for the 10.5:1 CR case as a function of RON and sensitivity are shown in Fig. 2. The complete set of maps is shown in [3].

The benefits of high sensitivity on efficiency are particularly visible for the 92 RON fuels. At high speed/low load points. Focusing on the region around 1500 rpm/16 bar IMEP, it is found that the efficiency clearly increases with increased sensitivity. There is still an increase in efficiency with sensitivity at higher speeds, suggesting a negative K value across the map, so that higher fuel sensitivity means a higher OI from Eq. 2.

The benefits of higher sensitivity are less apparent for the 98 RON base fuels. It has been found previously that the incremental benefits of higher OI fuels decrease as the OI increases [2].

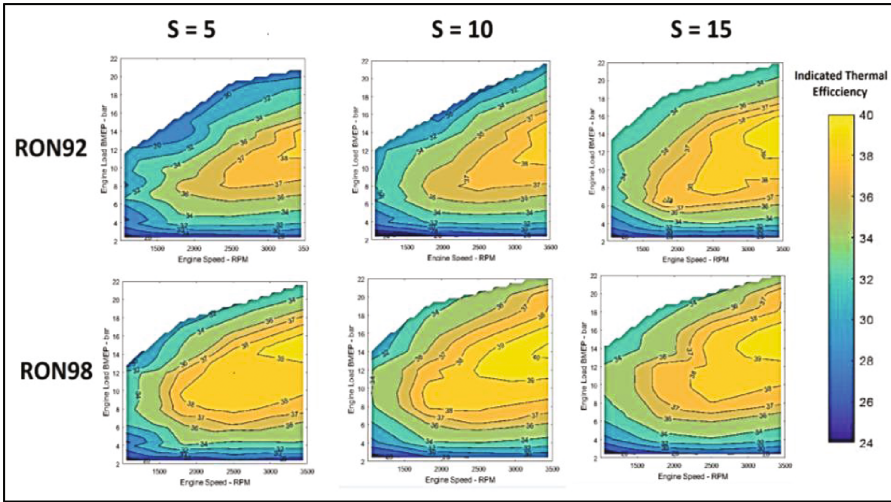


**Fig. 2.** Indicated thermal efficiency versus speed and load for CR 10.5:1 as a function of RON and sensitivity.

A more detailed analysis of this data set in [18] shows clearly that K value decreases with engine load and also suggests a more negative K value with increased compression ratio. This data does not reveal a clear dependence on engine speed, although as previously noted, several studies have shown that K value increases with engine speed.

### 3 Chemical Kinetic Interpretation of K Value Dependence on Speed and Load

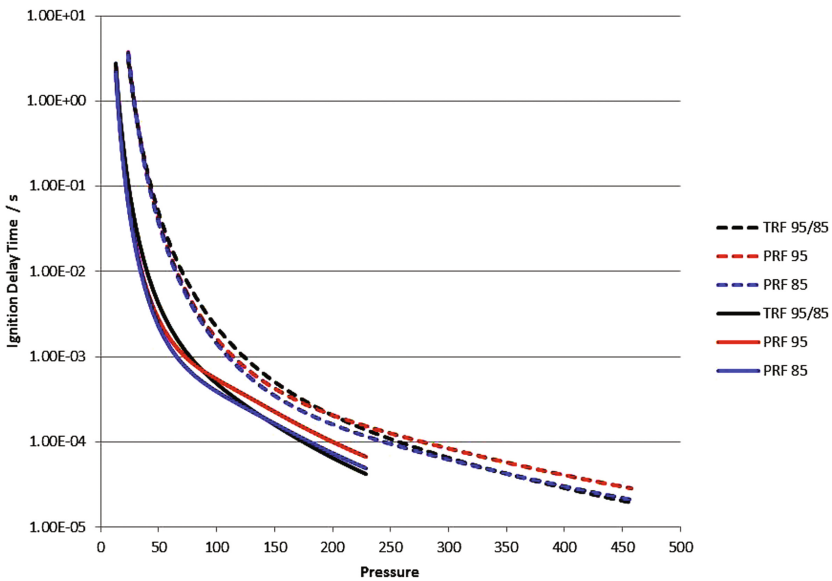
The chemical kinetic modelling studies shown in Fig. 1 have been extended in order to explore the impact of speed and load on K value. Two major assumptions have been used in this analysis:

1. The pressure and temperature of the end gas (both in the compression stroke before the spark and after the spark) are related to each other by a compression isentrope of constant gamma (we assumed a value of  $\gamma = 1.26$ ). This means that any heat transfer effects are ignored.
2. The point at which auto-ignition of the end-gas occurs can be predicted by the crank angle position at which Livengood-Wu integral [17] reaches unity,

$$\int_{t_i}^{t_f} \frac{1}{\tau(T,p)} dt = 1, \tag{3}$$

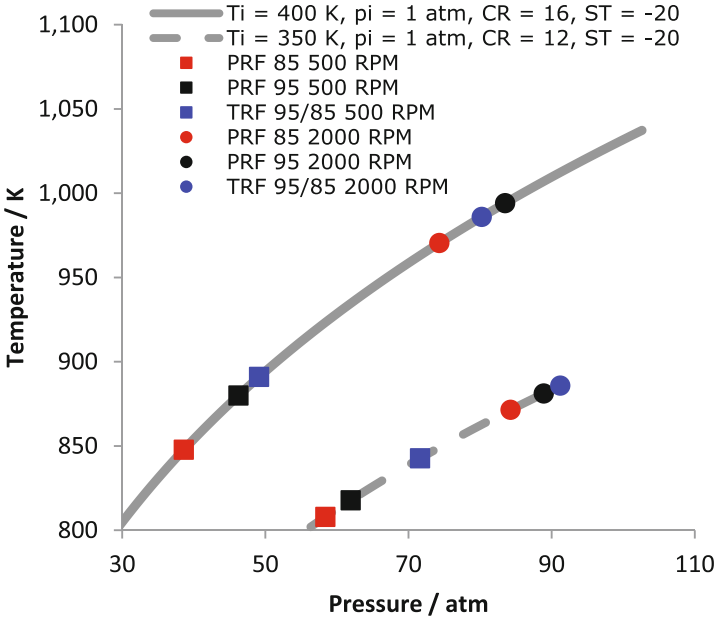
where t is time and  $\tau(T,p)$  ignition delay time under a constant temperature, T and pressure, p predicted by the chemical kinetic model. The pressure is estimated by a simple 0D engine model which represents the combustion by a Wiebe function.

Figure 3 shows autoignition delay times for the fuels described in Fig. 1, modelled by the Andrae mechanism [8], plotted as a function of pressure, where pressure and temperature are related to each other along a compression isentrope for each fuel. The curve contains similar features to Fig. 1: At the lower  $p$  and  $T$  region of the TRF 95/85 is more resistant to autoignition than PRF 85. The question of where the LWI will have reached unity is critical: If autoignition occurs before the cross over point of the blue and black lines then the  $K$  value is negative, otherwise the  $K$  value is positive. Obviously changing the starting conditions will change the isentrope. An initial pressure of 2 atm., and the same intake pressure, will shift the curve to the right. Even though the pressures are higher, the ignition delay times are longer because the temperature for a given pressure is lower.



**Fig. 3.** Ignition delay time plotted against pressure along compression isentropes for each fuel [Air intake pressure = 1 atm (solid lines) 2 atm (dashed lines), Air intake temperature = 300 K,  $\phi = 1$ ].

Changing the engine speed does not alter the isentrope. It is just that with a higher engine speed, the time elapsed per crank angle degree diminishes, and higher values of  $p$  and  $T$  are reached before the Livengood Wu Integral reaches unity. This is illustrated by Fig. 4, which shows 2 different compression isentropes. The  $p$  and  $T$  history was related to crank angle using a simple 0D model. The compression ratio (CR) and spark timing (ST) do not affect the locus of the isentrope, but the spark timing will influence the rise of the end gas pressure, which will affect the position on the isentrope where the Livengood Wu integral reaches unity.



**Fig. 4.** Values of  $T$  and  $p$  at which autoignition occurs (defined by when the Livengood-Wu integral reaches unity) at different RPM values and initial conditions.  $p_i = 1$  atm.  $\phi = 1$ . Solid line:  $T_i = 400$  K, Dash line:  $T_i = 350$  K. Black symbols represent PRF 95, red symbols represent PRF 85 and the blue symbols represent the surrogate “realistic” gasoline with 95 RON and 85 RON with composition described in the legend to Fig. 1.

Looking at the solid line in Fig. 4, representing the initial conditions of 1 atm and 400 K, for the case of 2000 RPM represented by the filled circles, it can be seen that the Livengood Wu integral reaches unity at a higher  $T$  and  $p$ , for the PRF 95 fuel (black point) than the TRF85/95 which in turn reaches unity at a higher  $p$  and  $T$  than PRF 85. Thus, the TRF95/85 fuel would knock at a point that is intermediate in crank angle, between the PRF85 and PRF95 fuels. The  $K$  value under these conditions would therefore be in the range between 0 and 1. However for the 500 rpm case, represented by the filled squares, the TRF95/85 fuel is actually more resistant to knock than PRF95, suggesting a negative  $K$  value. An increase in engine speed appears to be associated with an increase in  $K$  value.

The isentrope which passes through 1 atm and 350 K (dashed line) represents the situation with a pressure/temperature trajectory associated with a higher air intake pressure and a higher load. The TRF95/85 fuel is more resistant to auto ignition than the PRF95 fuel at both 500 rpm and 2000 rpm suggesting a negative  $K$  value under all these conditions. The extent to which the  $K$  value is negative can be visualised by the distance along the isentrope in  $T, p$  space between the point at which the TRF 85/95 fuel autoignites (i.e. with a Livengood Wu integral reaching unity) and the point at which the PRF95 fuel autoignites. This suggests both that the  $K$  value does indeed increase with rpm and decreases with load.



Note that the model does not include heat loss or friction and is just intended to illustrate trends. The rpm values chosen do not represent a real engine, but do illustrate the trends that would be observed. The effect of heat loss could be approximated by modelling the compression using a polytropic coefficient ( $1 < n < \gamma$ ) and would lead to a lower temperature for a given pressure, which would give a directionally lower K value.

## 4 Conclusion

Six E10 fuels with two different levels of RON and three octane sensitivity (RON-MON) levels were used to investigate how fuel octane quality can impact efficiency in modern DISI engines. Efficiency gains as a function of octane sensitivity are shown across the speed/load range. The way in which sensitivity affects anti-knock quality can be quantified by a K value, where the octane index is given by  $OI = RON - K \times S$ . A negative value of K suggests that high sensitivity will be beneficial.

In a complementary study, chemical kinetic modelling, combined with a 0D engine model was used to determine how the K value of an engine will vary with the locus of the p, T isentrope and with engine speed. As expected the model shows that that the cooler the end-gas temperature is (for a given pressure) the more negative the K value. It also shows that K increases with engine speed in agreement with several reported studies.

**Acknowledgement.** Funding from the European Commission Marie Curie Transfer of Knowledge Scheme (FP7) pursuant to Contract PIAP-GA-2013-610897 GENFUEL is greatly acknowledged.

## References

1. Prakash, A., Cracknell, R., Natarajan, V., Doyle, D., Lobato, P., Hinojosa, M.: Understanding the Octane Appetite of Modern Vehicles. SAE Technical Paper 2016-02-0834 (2016)
2. Redmann, J., Beutler, M., Kensler, J., Luebbers, M., et al.: Octane Requirement and Efficiency in a Fleet of Modern Vehicles. SAE Technical Paper 2017-01-0810 (2017). <https://doi.org/10.4271/2017-01-0810>
3. Prakash, A., Wang, C., Janssen, A., Aradi, A., et al.: Impact of Fuel Sensitivity (RON-MON) on Engine Efficiency. SAE Technical Paper 2017-01-0799 (2017)
4. Remmert, S., Campbell, S., Cracknell, R., Schuetze, A., et al.: Octane appetite: the relevance of a lower limit to the MON specification in a downsized, highly boosted DISI engine. SAE Int. J. Fuels Lubr. **7**(3), 743–755 (2014). <https://doi.org/10.4271/2014-01-2718>
5. ASTM: D2699 - Standard Test Method for Research Octane Number of Spark-Ignition Engine Fuel. American Society for Testing and Materials (2013)
6. ASTM: D2700 - Standard Test Method for Motor Octane Number of Spark-Ignition Engine Fuel. American Society for Testing and Materials (2011)
7. Morgan, N., Smallbone, A., Bhave, A., Kraft, M., Cracknell, R.F., Kalghatgi, G.K.: Mapping surrogate gasoline compositions into RON/MON space. Combust. Flame **157**, 1122–1131 (2010)

8. Andrae, J.C.G.: Comprehensive chemical kinetic modeling of toluene reference fuels oxidation. *Fuel* **107**, 740–748 (2013)
9. Kalghatgi, G.: Fuel Anti-Knock Quality - Part I. Engine Studies. SAE Technical Paper 2001-01-3584 (2001)
10. Kalghatgi, G.T.: Fuel anti-knock quality-Part II: Vehicle Studies-how relevant is Motor Octane Number (MON) in modern engines. SAE Technical Paper 2001-01-3585 (2001)
11. Szybist, J.P., Splitter D.A.: *Combustion and Flame* **177**, 49–66
12. Orlebar, C.N., Joedicke, A., Studzinski, W.: The effects of octane, sensitivity and K on the performance and fuel economy of a direct injection spark ignition vehicle. SAE Technical Paper 2014-01-1216 (2014)
13. Mittal, V., Heywood, J.: The shift in relevance of fuel RON and MON to knock onset in modern SI engines over the last 70 years. *SAE Int. J. Engines* **2**(2), 1–10 (2010)
14. Davies, T., Cracknell, R., Lovett, G., Cruff, L., et al.: Fuel Effects in a Boosted DISI Engine. SAE Technical Paper 2011-01-1985 (2011)
15. Zhou, Z., Yang, Y., Brear, M., Lacey, J., et al.: A comparison of four methods for determining the octane index and K on a modern engine with upstream, port or direct injection. SAE Technical Paper, 2017-01-0666 (2017)
16. Kassai, M., Shiraishi, T., Teraji, A., Wakefield, S., Goh, T., Doyle, D., Wilbrand, K., Shibuya, M.: The Effect of fuel properties on knocking performance of boosted downsized engines. In: Presented at the International Conference on “Advanced Fuels for Sustainable Mobility”, 4th–5th November 2014
17. Livengood, J.C., Wu, P.C.: Correlation of autoignition phenomena in internal combustion engines and rapid compression machines. *Symp. Combust. Proc.* **5**(1), 347–356 (1955)
18. Wang, C., Prakash, A., Aradi, A., Cracknell, R.F., Xu, H.: Significance of RON and MON to a modern DISI engine. *Fuel* **209**, 172–183 (2017)